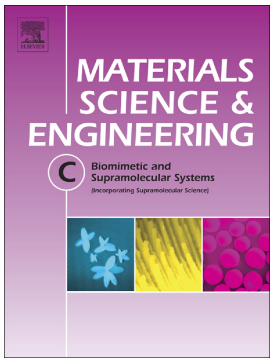

Calcium silicate layer on titanium fabricated by electrospray deposition

Csaba Buga, Mátyás Hunyadi, Zoltán Gácsi, Csaba Hegedűs, József Hakl, Ute Schmidt, Shinn-Jyh Ding, Attila Csík

PII: S0928-4931(18)32187-8
DOI: https://doi.org/10.1016/j.msec.2019.01.011
Reference: MSC 9269

To appear in: *Materials Science & Engineering C*

Received date: 24 July 2018
Revised date: 2 January 2019
Accepted date: 3 January 2019

Please cite this article as: Csaba Buga, Mátyás Hunyadi, Zoltán Gácsi, Csaba Hegedűs, József Hakl, Ute Schmidt, Shinn-Jyh Ding, Attila Csík , Calcium silicate layer on titanium fabricated by electrospray deposition. Msc (2018), https://doi.org/10.1016/j.msec.2019.01.011

Calcium silicate layer on titanium fabricated by electrospray deposition

Csaba Buga[a], Mátyás Hunyadi[a], Zoltán Gácsi[a], Csaba Hegedűs[b], József Hakl[a], Ute Schmidt[c], Shinn-Jyh Ding[d,e,*], Attila Csík[a,*]

[a]Institute for Nuclear Research, Hungarian Academy of Sciences (ATOMKI), H-4026 Debrecen, Bem tér 18/C, Hungary

[b]Department of Biomaterials and Prosthetic Dentistry, Faculty of Dentistry, University of Debrecen, H-4032 Debrecen, Egyetem tér 1, Hungary

[c]WITec GmbH, Lise-Meitner-Str. 6, D-89081 Ulm, Germany

[d]Institute of Oral Science, Chung Shan Medical University, Taichung City 402, Taiwan

[e]Department of Stomatology, Chung Shan Medical University Hospital, Taichung City 402, Taiwan

* Corresponding author:

Shinn-Jyh Ding

Institute of Oral Science, Chung Shan Medical University, Taichung City 402, Taiwan

Tel.: +886-4-24718668 ext. 55529

Fax: +886-4-24759065

E-mail address:sjding@csmu.edu.tw

Attila Csík

Institute for Nuclear Research, Hungarian Academy of Sciences (ATOMKI), Debrecen, Hungary

Tel.: +36 52 509 212

Fax.: +36 52 416 181

E-mail address: csik.attila@atomki.mta.hu

Abstract

Titanium and its alloys have been used as implant materials. Non-ideal osseointegration of the implant materials has facilitated the development of the bioactive coatings on the implant surfaces. In this work, the bioactive calcium silicate (CaSi) powder prepared in a green synthesis route was used to cover the surface of Ti implants by a facile electrospray deposition method. Post annealing in air was also applied to form the oxidation layer on the Ti surface with the aim of increasing the bond strength between the CaSi coating layer and Ti substrate. For the characterization of the coatings several analytical methods such as X-ray diffraction, scanning electron microscopy, secondary neutral mass spectrometry, and Raman-spectroscopy were used, in addition to the measurement of bond strength and corrosion resistance. The results indicated a uniform CaSi layer with a thickness of about 1 μm deposited on the Ti substrate. Annealing in the range of 700–900 °C in air resulted in the formation of rutile phase of TiO_2; more importantly, annealing at 800 °C did not significantly affect the composition of the CaSi layer consisting of β-Ca_2SiO_4. The bond strength between the coating layer and Ti substrate can be remarkably enhanced at an annealing temperature of 700 or 800 °C compared with the as-prepared coating without annealing. The annealed coatings had a better corrosion resistance than the as-prepared coating. It is concluded that the electrospray method associated with the post-annealing can be successfully used for the deposition of a CaSi layer with a defined structure and composition on titanium implants.

Keywords: calcium silicate; bioactive coating; electrospray deposition; annealing

1. Introduction

Titanium and its alloys (e.g., Ti–6Al–4V) are the most commonly used implant materials for dental and orthopedic applications because of their good mechanical properties and biocompatibility. Despite the desirable properties of titanium, the direct structural and functional connection between the living bone and the implant surface usually occurs in 3–4 months and occasionally is not effective [1]. If osseointegration does not occur in a specific period of time, it may result in improper bonding of the implants to bone tissues and finally lead to implant failure [2]. Thus, the high bioactivity of the metallic implant plays an important role in a long-term implantation success. The characteristics of the implant surface dominate the biological response to bone tissues, which would lead to develop the surface treatments of titanium implants.

Surface treatments of titanium (e.g., sandblasting, chemical and electrochemical etching, and anodic oxidation) are always selected to stimulate a direct bond between the implant surface and tissues [3]. Beyond the surface treatments, bioactivity of implants can be greatly enhanced if the implant surface is covered with a bioactive layer [4–7]. Thus, much effort has been made to develop bioactive coatings on metallic substrates using a variety of methods. To achieve good biological properties of the coated implant, the bioactive layers must have adequate composition, molecular, and crystal structure. Although such methods as plasma spraying, sputtering, and sol-gel are widely used for surface modification [4,8–10], recently the electrospray deposition (ESD) is received much attention because of its simplicity, effective and economical process [11]. It is an effective method to deposit thin-film layer with defined morphological and chemical characters in a fast way at room temperature. The basic principle of working is the generation of charged spray with micron-sized liquid particles, which is accomplished by the electrostatic atomization of precursor solutions [12]. These spray droplets are directed toward to the grounded substrate as a result of the applied potential

difference and can form a compact layer even in micrometers of thickness. For example, calcium phosphate [13] and zin oxide [14] are deposited on the substrates by ESD.

Given that calcium is a potent regulator of cell behaviour and has significant effects on the proliferation and differentiation of osteoblasts, calcium-based biomaterials can form a strong bond with the surrounding bone tissue under clinical conditions [15,16]. In addition to calcium, silica on the surface of titanium can also enhance attachment and mineralization of osteoblast-like cells [6]. The calcium silicate (CaSi)-based materials can expedite the differentiation of the human mesenchymal stem cells [17]. On the other hand, CaSi ceramics show greater ability to support cell attachment, proliferation, and differentiation than β-tricalcium phosphate (β-TCP) ceramics [18]. More bone formation is observed with calcium silicate as compared to β-TCP in reconstruction of the rabbit calvarial defects [19]. Hence, CaSi can be used as a coating material on the titanium surface because of its higher osteogenesis [20–22]. A $CaSiO_3$ coating with a sheet-like nano-structure on the Ti–6Al–4V substrate is fabricated by a combination of atmosphere plasma spraying and hydrothermal technology [23]. The applications of CaSi-based materials instead of calcium phosphate on Ti implants are more promising and would be used as a bone replacement material in restorative dental and orthopedic implants. The plasma-sprayed Ca_2SiO_4 coatings disclose good bioactivity and enhanced bonding strength with Ti–6Al–4V [24]. The bioactive $CaSiO_3$ coating is deposited on Ti substrates by oxyacetylene flame spraying, which shows an elastic modulus similar to that of the cortical bone [25].

As previously mentioned, the electrospray deposition can be used to deposit a thin ceramic film with a defined surface structure and composition. In addition, very simple set-up and high deposition efficiency are another advantage of the ESD technique [13]. To our knowledge, there have been few previous studies on the investigation of electrosprayed CaSi coatings. In this study we presented the applicability of the ESD method at room temperature

for coating of polished Ti plates with CaSi powder prepared in green synthesis route. Post-annealing in air has been applied to form an oxide phase, with the aim of increasing the bond strength of the coating to the polished titanium surface. Analytical methods such as scanning electron microscope (SEM), X-ray diffraction (XRD), secondary neutral mass spectrometry (SNMS), and Raman spectroscopy were used for structure and composition analysis of the coatings before and after annealing, in addition to examination of the bond strength and corrosion resistance.

2. Materials and methods

2.1. Preparation of powder suspension

In this work we used the CaSi powder with Ca:Si=7:3 ratio for spraying experiments. The green synthesis via the hydrothermal method for the preparation of the CaSi powder can be found elsewhere [26]. Briefly, reagent grade tetraethyl orthosilicate (TEOS; Sigma-Aldrich, St. Louis, MO, USA) and calcium nitrate (Showa, Tokyo, Japan) were used as precursors for SiO_2 and CaO, respectively. Solutions of TEOS and calcium nitrate in water were placed in a Teflon vessel that was heated to a temperature of 120 °C holding for 1 day in an oven and then allowed to cool naturally to room temperature. The vaporization of the solvent was performed in an oven at 120 °C. The final CaSi powder was obtained by sintering the dried gel at 800 °C in air for 2 h at a heating rate of 10 °C/min using a high-temperature furnace, followed by cooling to room temperature in the furnace. The sintered granules were ball milled for 12 h in ethanol using a centrifugal ball mill (Retsch S 100, Haan, Germany) and then dried in an oven at 60 °C. For electrospray deposition the CaSi powder (150 mg) was suspended in 14 mL of ethanol and ultrasonic bath was used to increase homogeneity. After 1 h sedimentation the supernatant fraction was used as the suspension for deposition of CaSi layer on the Ti substrate. To understand the structure of the suspension, it was placed in a

metallic holder for evaporation of ethanol, and then the dried sediment was observed under a SEM (Hitachi S-4300, Tokyo, Japan).

2.2. Preparation of substrate and coating

Commercially available grade 2 titanium plates (Spemet Co., Taipei, Taiwan) of 10×10×1 mm^3 were selected as the coating substrate. Prior to electrospray, the substrate surface was mechanically polished to #1500 grit level, followed by using 1-μm alumina suspension on polishing cloths to produce a smooth surface advantageous to the structural observation and elemental depth profile analysis. The substrates were then etched in 30% HNO_3 for 30 min at room temperature, followed by ultrasonic cleaning in ethanol for 30 min, rinsing with distilled water for 30 min and air drying. ESD was then used to cover the polished Ti plates with the CaSi suspension, as schematically presented in Fig. 1. Deposition process was performed at room temperature and a stainless steel nozzle was used to produce the spray. The experimental conditions were set-up after some preliminary trials. The CaSi suspension was pressed through the nozzle with syringe pump at a flow rate of ~1.25 μL/sec. The negative high voltage of 4.5 kV was applied between the nozzle and Ti plates. After that, the as-prepared coatings were annealed for 30 min in air at different temperatures (500–900 °C) with a heating rate of 10 °C/min, and then cooled to room temperature in the furnace to improve the bonding of coatings to the smooth substrates, according to a previous study [27].

2.3. Morphology and composition

Surface morphology and composition of layers before and after annealing were analysed by SEM equipped with energy dispersive X-ray (EDX) analyzer. To obtain crystallographic information from the coating with and without annealing, the X-ray diffraction measurements were performed by Siemens Kristalloflex 710H diffractometer (Karlsruhe, Germany) using

CuKα irradiation with wavelength λ=0.154 nm operating at 40 mA and 40 kV. Raman measurement (alpha300, WITec GmbH, Ulm, Germany) was done by using a 532 nm excitation laser with 20 mW of power. A secondary neutral mass spectrometer (SMNS; INA-X, SPECS GmbH, Berlin, Germany) was used for the depth profiling of the specimens, which can be used for the calculation of the thickness values of the coating layer and oxidation layer. Three replicates were carried out for each group, and the results were expressed as the mean ± standard deviation. The surface roughness values (R_a) at ten different areas on samples were determined using Ambios XP-I stylus profiler. The 2-mm scan length was chosen for measurement with 1 mg of stylus load force and 0.1 mm/sec scan speed.

2.4. Bond strength

Bond strength (or adhesion strength) was used to simply represent the present pull-out test results of the various coatings using an EZ-Test machine (Shimadzu, Kyoto, Japan) at a crosshead speed of 0.5 mm/min. While doing the testing, a 2.7-mm diameter aluminum pull stud (Quad Group, Spokane, WA) was bonded to the coated surface with epoxy; it was then cured at 150°C for 1 h in an oven. After the coated specimen/stud assembly was gripped on a platen, the stud was then pulled down against the platen until failure occurred [28]. The maximum fracture force can be recorded and averaged to obtain the mean value and standard deviation. The number of measurements was five for each group.

2.5. Corrosion measurement

The corrosion measurements included open circuit potential (OCP) time methods and potentiodynamic polarization in a simulated body fluid (SBF) solution, using a CHI 660A electrochemical system (CH Instrument, Austin, TX, USA). The SBF solution, the ionic composition of which is similar to that of human blood plasma, consisted of 7.9949 g NaCl,

0.3528 g $NaHCO_3$, 0.2235 g KCl, 0.147 g K_2HPO_4, 0.305 g $MgCl_2 \cdot 6H_2O$, 0.2775 g $CaCl_2$, and 0.071 g Na_2SO_4 in 1000 mL distilled H_2O and was buffered to pH 7.4 with hydrochloric acid (HCl) and tris-hydroxymethyl aminomethane (Tris, $(CH_2OH)_3CNH_2$) [6]. All chemicals used were of reagent grade and used as obtained. For OCP measurement, only two electrodes (working electrode and reference electrode) were involved, whereas for the potentiodynamic polarization method, a conventional three-electrode cell was used. A saturated calomel reference electrode (SCE) and a platinum counter electrode were employed. The sample surface was cleaned by distilled water. The evaluation of potentiodynamic polarization was started after soaking in SBF for 1 h. The scanned potential range varied from −1 to 1 V toward the anodic direction at a sweep rate of 1 mV/s in the Tafel mode. The current was recorded in the absence of stirring or gas bubbling into the electrolyte. The corrosion potential and corrosion current density were provided after being analyzed by the software. The results were obtained from five separate experiments.

2.6. Statistical analysis

One-way analysis of variance (ANOVA) was used to evaluate significant differences between means in the measured data. Scheffe's multiple comparison testing was applied to determine the significance of the standard deviations in the measured data from each specimen under different experimental conditions. In all cases, the results were considered statistically significant with p-values less than 0.05.

3. Results and discussion

3.1. Morphology of the used suspension

One way for increasing the bioactivity and reducing the implantation failure of Ti implants is to coat the metallic surface by a bioactive layer. The purpose of the current work

was the preparation of a bioactive CaSi layer on Ti surface by ESD. First of all, it necessitated to demonstrate the morphology of the CaSi suspension used for the electrospray deposition process. As it can be seen in the Fig. 2, the particles with size of few nanometers were agglomerated into the 1-2 μm clusters, in consistent with the previous report [26].

3.2. Morphology and composition of the as-prepared coatings

Fig. 3a shows the SEM picture taken from the surface of a Ti substrate after deposition of CaSi layer without post-annealing. The electrospray deposition produced a uniform coverage of the Ti substrate with CaSi. Higher magnification analysis revealed that the layer consisted of granules with sizes similar to the morphology of the used suspension. EDX analysis indicated the Ca/Si ratio (2.32 ± 0.19) of the deposited layer, which was in good agreement with original Ca/Si ratio (7/3 = 2.33) of the used powder (Fig. 3b).

XRD and Raman spectroscopy analysis of the as-prepared coating showed typical peaks of Ti and β-Ca_2SiO_4 (β-dicalcium silicate) (Fig. 4). We can see the two strongest lines of Ti (38.6^o and 40.4^o) in the XRD pattern (Fig. 4a). In addition, the diffraction peaks at 2θ values between 32° and 34° were attributed to the β-Ca_2SiO_4 phase [26]. In the Raman spectrum (Fig. 4b), the typical peaks ranging from 750 to 900 cm^{-1} were ascribed to the Ca_2SiO_4 phase [29], whereas peaks in range of less than 400 cm^{-1} corresponded to the lattice vibrations of Ca–O [30]. ESD allows strong control over deposition parameters such as coating thickness, surface morphology and composition since the liquid phase is a discontinuous aerosol instead of a continuous bulk liquid phase [31]. As expected, the currently used ESD did not affect the morphology and composition of the used powder, which was one of the purposes in this study.

3.3. Composition and morphology of the annealed coatings

The XRD results showed that annealing in air at 500 °C cannot cause any remarkable changes in the phase composition (Fig. 5). However, after annealing at 600 °C the major peak of rutile at 2θ = 27.44° appeared, the main peaks of Ti were slightly reduced. In addition, the main peaks related to the β-Ca_2SiO_4 phase at 2θ = 32–34^o were still remained. In the case of 700 °C the peaks of the rutile phase appeared more significantly, because of the increasing thickness of the oxidation layer, but the diffraction intensity of β-Ca_2SiO_4 phase was also noticeable. Two small peaks became visible at the position of 29° and 31.5°, which were identified as Ca_3SiO_4 and $CaSiO_3$, respectively. By further increase of annealing temperature to 800 °C, the formation of new Ca-Si-O phases and growing rutile-TiO_2 phase were more remarkable, with the remaining β-Ca_2SiO_4. Finally, at an annealing temperature of 900 °C the original peaks of the β-Ca_2SiO_4 phase disappeared, indicating that this phase was completely transformed into the other two CaSi phases. It can be noted that we cannot observe the formation of the anatase phase, since its major peak at 2θ = 25.28° was not found for any of the annealed samples. This is in good agreement with literature that no anatase could be formed by thermal oxidation of Ti in air [27,32].

The surface morphologies of a series of annealed coatings at different temperatures are shown in Fig. 6. The annealing at 500–700 °C did not change the surface morphology, revealing very similar appearance to the as-prepared CaSi coating. In contrast to the findings, the large particles appeared on the surface of the 800 °C-annealed coating, possibly due to the grain growth and phase transformation, consistent with XRD results. As a general trend, an increase of the particle size was observed for 900 °C-annealed coating surface, which could result in the rough surface. The roughening of the surface can also be visually observed and confirmed by the surface roughness measurement. For polished Ti substrate the surface roughness (R_a) has been determined as 290±37 nm, while the as-prepared coating was 341±30

nm. After annealing at 800 °C, the Ra value increased significantly ($p < 0.05$) to 410±28 nm compared with the Ti control and as-prepared coating, which was congruent with the results of SEM showing the variations in the particle sizes. It is speculated that the increased surface roughness would be beneficial for osseointegration.

To further clarify the effect of annealing, the cross-sectional SEM image of the 800 °C-annealed sample showed the formation of an approximately 1–2 μm-thick oxidation layer, as shown in Fig. 7a. Moreover, a continuous structure between the deposited CaSi particles and the oxidation layer might be formed, possibly because of the partial melting of nano-structured CaSi cluster. The continuous structure might induce a chemical or mechanical bonding at the coating-oxidation layer interface. The adhesion between the coating and substrate depends on the mechanical interlocking and the chemical bonding [33]. It left no doubt that the firm bonding was beneficial for enhancing the bond strength, as stated in strength results below.

3.4. Thickness of the coatings

To get more information, the SNMS depth profile of all annealed coatings was performed. Because of the high surface roughness it was not possible in this measurement to reach the optimal depth resolution (the interface boundaries between the layers did not show a sharp profile), nevertheless the range of the individual layers can be assigned. The 800 °C-annealed coating was used as an example to demonstrate the determination of thickness, as shown in Fig. 7b. The thickness of the layers was determined by applying a following procedure: (1) the width of the interface (Δx) between the two layers including the CaSi coating (d_{Ca}) and the oxidation film (d_{TiO}) can be measured as the distance corresponding to the 90 to 10% decay (or increase) of measured intensity; (2) the 50% of the determined width can be defined as the position of the interface between two layers [34,35]. The SNMS results

indicated that the 800 °C-annealed CaSi layer had a coating thickness of about 1 μm. The oxidation layer with a thickness of about 2 μm on the surface of Ti substrate was clearly found, which reflected the consequence of annealing in air. Interestingly, a large overlapping in the depth profile between the CaSi coating and Ti component was found, which was in line with the findings of the cross-sectional SEM image. In addition, the SNMS examination also showed that the mean of all CaSi coating thickness was roughly 1 μm with small scattering before and after annealing (Table1). This result may be interpreted by the use of smooth substrates. No statistical difference ($p > 0.05$) implied the annealing temperature-independent coating thickness, although the annealing can promote the grain growth and phase transition as demonstrated previously by the results of SEM and XRD. It is well-known that the thickness of a native oxide layers is about 5–10 nm on Ti [36]. After annealing at 500 °C to 900 °C, the thickness of the oxidation layer significantly ($p < 0.05$) increased from 57 nm to 4742 nm, respectively. Similar to the findings by Velten et al. [37], the thickness of the oxidation layers on the polished titanium surface was as a function of thermal oxidation temperature, which the thickness values were about 60 nm and 200 nm after thermal treatment at 500 °C and 600 °C for 40 min, respectively. By elevating the temperature, the oxidation layer on the titanium surface usually gets thicker because of oxygen internal diffusion from the surface to form the ordered phases [38], in agreement with the evolution of XRD.

3.5. Bond strength

Despite the favorable structural properties, assessment of bond strength is an important first step for successful implant applications. It should examine the effect of the post-annealing on the bonding strength of the coating to the smooth Ti substrate in order to clarify bonding efficacy of the protective and adherent oxidation layer. From the aforementioned XRD, SEM, and SNMS results, annealing at 700 °C can effectively promote the growth of the

oxidation layer, while annealing at 900 °C led to a thick rutile layer. Thus, the coated samples annealed at 700, 800, and 900 °C were used to test the bond strength, along with the as-prepared coating. The measured bond strength value of the as-prepared coating was 2.6±0.6 MPa (Table 1). When subjected to different annealing temperatures, the strength value became 7.0±3.1, 9.5±2.9, and 2.5±0.3 MPa for samples annealed at 700, 800, and 900 °C, respectively. The bond strength values for samples annealed at 700 and 800 °C were significantly ($p < 0.05$) higher than that of the as-prepared coating. A potential mechanism responsible for this strength increase can be understood as a suitable thickness (0.38–1.82 μm) of the formed oxidation layer that effectively promoted the chemical affinity between the underlying titanium and the upper ceramic layer. According to the literature [39,40], titanium oxide can be used as a bond layer for improving the bond strength of coatings to metallic substrate. Nevertheless, when annealed at higher temperature such as 900 °C, the excessive thickness (e.g., 4.75 μm) of the oxidation layer near the titanium substrate may result in poor adhesion, in turn, detrimental to the bonding, although possessing a higher crystallinity of rutile phase. An optimal oxidation layer thickness formed on the titanium surface plays an important role in metal-ceramic bonding, consistent with a previous study [27]. Dai et al. [38] suggested that at lower temperature, a compact oxidation layer formed by Ti and oxygen can completely cover the metallic surface. However, because the activity and diffusion velocity of oxygen become strong at higher temperature, the layer turns to a loose and porous structure, which the thicker oxidation layer weakens the bond strength between the layer and the substrate, resulting in spalling from the substrate. In this work, the obtained bond strength was lower than that of the ISO 13779 standard (15 MPa) [41]. As references for using plasma spraying on sandblasted surfaces, the bond strength values of CaSi coatings are in the range of 20–40 MPa [23,24]. Since the factors for the success of ceramics-metal bonding may include interfacial chemistry, interfacial morphologies, and mechanical stresses [42], it is reasonable

to use roughened Ti substrates for improving the bond strength by means of mechanical interlocking, which will be the focus of the future work. For example, Pourhashem and Afsharn [43] reported that the bond strength (3 MPa) of CaSi-based glass coating on sandblasted 316L stainless steel substrates using the sol-gel method was higher than that (0.5 MPa) on polished substrates.

3.6. Corrosion behavior

The as-prepared and annealed samples at 700, 800, and 900 °C were used for corrosion measurement, in addition to the Ti control without coating. In order to evaluate the corrosion behavior of the coating implants, the changes in OCP over time of the samples in SBF are demonstrated in Fig. 8. It can be clearly seen that OCP of the all samples shifted towards a steady state after soaking in SBF. Compared to the Ti control, the coating samples showed a higher initial potential and attained more noble potential values, indicating a superior corrosion behavior. Among the coating samples, the annealed samples exhibited a better corrosion resistance during the OCP measurements than the as-prepared sample by virtue of more noble potential. On the other hand, the differences in OCP between annealed coatings were not remarkable, which can be due to the oxidation layer formed during the annealing. The titanium oxide layer on the Ti substrate is a protective layer to reduce the occurrence of corrosion [44].

Typical potentiodynamic polarization curves are presented in Fig. 9. The measured corrosion potential and corrosion current density of all coating samples were obtained using Tafel extrapolation methods, as listed in Table 1. For the corrosion potential, the value of the as-prepared coating was −595±83 mV versus SCE, which was not significantly different from the Ti control (−567±39 mV). By contrast, the values of the annealed samples ranged from −431 to −345 mV, indicating no significant difference ($p > 0.05$) between the annealed

samples. The shifting of corrosion potential of the materials towards more positive values demonstrated a greater corrosion-resistant ability. Interestingly, the statistical analysis revealed a significant difference ($p < 0.05$) between the as-prepared sample and annealed samples. This can be explained by the fact that the weak bonding of the as-prepared coating on the smooth Ti substrate might lead to the worse corrosion-resistant ability. The corrosion rate of a coating implant is related to the corrosion current density. The higher the current density value, the greater the corrosion rate is on the coating when exposure to SBF. The comparative study indicated the average values of the coating samples between 22 and 67 nA/cm^2, indicating no significant difference ($p > 0.05$) (Table 1). The Ti control had significantly higher ($p < 0.05$) current values (186 nA/cm^2) compared to the coating samples. The oxidation layer at the coating-substrate interface resulted in a significant increase in corrosion resistance of titanium.

4. Conclusions

The present study reported for the first time deposition of a homogeneous bioactive calcium silicate layer on the Ti substrate by a facile electrospray deposition. Annealing of deposited samples in the range of 700−800 °C in air was not only effective for the formation of a rutile phase of TiO_2, but also maintained the phase composition of the bioactive CaSi material. Of note, the post-annealing at temperature of 800 °C could achieve the significantly higher bond strength of 9.5 MPa as compared with the as-prepared coating (2.6 MPa), along with the enhanced corrosion resistance. The current investigation provided a simple and convenient method to form a uniform CaSi layer with a defined morphology and composition on Ti substrate. Further experiments are in progress to evaluate antibacterial activity, in vitro bioactivity and osteogenesis of the potential CaSi coating layer.

Acknowledgement

The work is supported by a Hungarian-Taiwan bilateral research program, No. NKM-75/2018 and MOST 106-2911-I-040-503. The XRD measurements were carried out in the frame of the GINOP-2.3.2-15-2016-00041 project, which is co-financed by the European Union and the European Regional Development Fund. The research is financed by the Higher Education Institutional Excellence Programme of the Ministry of Human Capacities in Hungary, within the framework of the Biotechnology thematic programme of the University of Debrecen. The publication is supported by the GINOP-2.3.2-15-2016-00011 project. The project is co-financed by the European Union and the European Regional Development Fund.

References

[1] R. Smeets, B. Stadlinger, F. Schwarz, B. Beck-Broichsitter, O. Jung, C. Precht, F. Kloss, A. Gröbe, M. Heiland, T. Ebker, Impact of dental implant surface modifications on osseointegration, BioMed Res. Int. 2016: 6285620.

[2] X. Chen, G. Chen, H. He, C. Peng, T. Zhang, P. Ngan, Osseointegration and biomechanical properties of the onplant system, Am. J. Orthod. Dentofacial. Orthop. 132 (2007) 278.e1–278.e6.

[3] X. Liu, P.K. Chu, C. Ding, Surface modification of titanium, titanium alloys, and related materials for biomedical applications, Mater. Sci. Eng. R: Reports 47 (2004) 49–121.

[4] K. de Groot, R. Geesink, C.P. Klein, P. Serekian, Plasma sprayed coatings of hydroxylapatite, J. Biomed. Mater. Res. 21 (1987) 1375–1381.

[5] H.J. Kim, Y.H. Jeong, H.C. Choe, W.A. Brantley, Surface characteristics of hydroxyapatite coatings on nanotubular Ti–25Ta–xZr alloys prepared by electrochemical deposition, Surf. Coat. Technol. 259 (2014) 274–280.

[6] C. Hegedűs, C.C. Ho, A. Csik, S. Biri, S.J. Ding, Enhanced physicochemical and biological properties of ion-implanted titanium using electron cyclotron resonance ion sources, Materials 9 (2016) 25;doi:10.3390/ma9010025.

[7] P. Petrov, D. Dechev, N. Ivanov, T. Hikov, S. Valkov, M. Nikolova, E. Yankov, S. Parshorov, R. Bezdushnyi, A. Andreeva, Study of the influence of electron beam treatment of Ti5Al4V substrate on the mechanical properties and surface topography of multilayer TiN/TiO_2 coatings, Vacuum 154 (2018) 264–271.

[8] E.S. Thian, J. Huang, M.E. Vickers, S.M. Best, Z.H. Barber, W. Bonfield, Silicon-substituted hydroxyapatite (SiHA): A novel calcium phosphate coating for biomedical applications, J. Mater. Sci. 41 (2006) 709–717.

[9] Y. Cai, S. Zhang, X. Zeng, Y. Wang, M. Qian, W. Weng, Improvement of bioactivity with magnesium and fluorine ions incorporated hydroxyapatite coatings via sol–gel deposition on Ti6Al4V alloys, Thin Solid Films 517 (2009) 5347–5351.

[10] C.C. Ho, S.J. Ding, Novel SiO_2/PDA hybrid coatings to promote osteoblast-like cell expression on titanium implants, J. Mater. Chem. B 3 (2015) 2698–2707.

[11] S. Kavadiya, P. Biswas, Electrospray deposition of biomolecules: Applications, challenges, and recommendations, J. Aerosol S. doi: 10.1016/j.jaerosci.2018.04.009, in press.

[12] N.A. Brown, Y. Zhu, G.K. German, X. Yong, P.R. Chiarot, Electrospray deposit structure of nanoparticle suspensions, J. Electrostat. 90 (2017) 67–73.

[13] S. Leeuwenburgh, J. Wolke, J. Schoonman, J. Jansen, Electrostatic spray deposition (ESD) of calcium phosphate coatings, J. Biomed. Mater. Res. 66A (2003) 330–334.

[14] K. Memarzadeh, A.S. Sharili, J. Huang, S.C.F. Rawlinson, R.P. Allaker, Nanoparticulate zinc oxide as a coating material for orthopedic and dental implants, J. Biomed. Mater. Res. 103A (2015) 981–989.

[15] M. Lin, L. Zhang, J. Wang, X. Chen, X. Yang, W. Cui, W. Zhang, G. Yang, M. Liu, Y. Zhao, C. Gao, Z. Gou, Novel highly bioactive and biodegradable gypsum/calcium silicate composite bone cements: from physicochemical characteristics to in vivo aspects, J. Mater. Chem. B 2 (2014) 2030–2038.

[16] W.S.W. Harun, R.I.M. Asri, J.Alias, F.H. Zulkifli, K. Kadirgama, S.A.C. Ghani, J.H.M. Shariffuddin, A comprehensive review of hydroxyapatite-based coatings adhesion on metallic biomaterials, Ceram. Int. 44 (2018) 1250–1268.

[17] S.C. Huang, B.C. Wu, S.J. Ding, Stem cell differentiation-induced calcium silicate cement with bacteriostatic activity, J. Mater. Chem. B 3 (2015) 570−580.

[18] S. Ni, J. Chang, L. Chou, W. Zhai, Comparison of osteoblast-like cell responses to calcium silicate and tricalcium phosphate ceramics in vitro, J. Biomed. Mater. Res. B 80 (2007) 174–183.

[19] S. Xu, K. Lin, Z. Wang, J. Chang, L. Wang, J. Lu, C. Ning, Reconstruction of calvarial defect of rabbits using porous calcium silicate bioactive ceramics, Biomaterials 29 (2008) 2588−2596.

[20] S.J. Ding, Y.H. Chu, D.Y. Wang, Enhanced properties of novel zirconia-based osteoimplant systems, Appl. Mater. Today 9 (2017) 622–632.

[21] F. Hao, L. Qin, J. Liu, J. Chang, Z. Huan, L. Wu, Assessment of calcium sulfate hemihydrate–Tricalcium silicate composite for bone healing in a rabbit femoral condyle model, Mater. Sci. Eng. C 88 (2018) 53–60.

[22] K. Lin, D. Zhai, Na. Zhang, N. Kawazoe, G. Chen, J. Chang, Fabrication and characterization of bioactive calcium silicate microspheres for drug delivery, Ceram. Int. 40 (2014) 3287–3293.

[23] X. Wang, Y. Zhou, L. Xia, C. Zhao, L. Chen, D. Yi, J. Chang, L. Huang, X. Zheng, H. Zhu, Y. Xie, Y. Xu, K. Lin, Fabrication of nano-structured calcium silicate coatings with

enhanced stability, bioactivity and osteogenic and angiogenic activity, Colloid Surf. B-Biointerfaces 126 (2015) 358–366.

[24] X. Liu, S. Tao, C. Ding, Bioactivity of plasma sprayed dicalcium silicate coatings, Biomaterials 23 (2002) 963–968.

[25] E. Garcia, P. Miranzo, M.A. Sainz, Thermally sprayed wollastonite and wollastonite-diopside compositions as new modulated bioactive coatings for metal implants, Ceram. Int. 44 (2018) 12896–12904.

[26] C.C. Chen, C.C. Ho, S.Y. Lin, S.J. Ding, Green synthesis of calcium silicate bioceramic powders, Ceram. Int. 41 (2015) 5445–5453.

[27] M. Yan, C.T. Kao, J.S. Ye, T.H. Huang, S.J. Ding, Effect of preoxidation of titanium on the titanium-ceramic bonding, Surf. Coat. Technol. 202 (2007) 288–293.

[28] S.J. Ding, Properties and immersion behavior of magnetron-sputtered multi-layered hydroxyapatite/titanium composite coatings, Biomaterials 24 (2003) 4233–4238.

[29] C. Remy, B. Reynard, M. Madon, Raman spectroscopic investigations of dicalcium silicate: polymorphs and high-temperature phase transformations, J. Am. Ceram. Soc. 80 (1997) 413–423.

[30] S. Ortaboy, J. Li, G. Geng, R. J. Myers, P.J. M. Monteiro, R. Maboudian, C. Carraro, Effects of CO_2 and temperature on the structure and chemistry of C–(A–)S–H investigated by Raman spectroscopy, RSC Adv. 7 (2017) 48925–48933.

[31] A.W. Nijhuis, S.C. Leeuwenburgh, J.A. Jansen, Wet-chemical deposition offunctional coatings for bone implantology, Macromol. Biosci. 10 (2010) 1316–1329.

[32] H. Zhang, J.F. Banfield, Thermodynamic analysis of phase stability of nanocrystalline titania, J. Mater. Chem. 8 (1998) 2073–2076.

[33] S. Zhang, Y.S. Wang, X.T. Zeng, K.A. Khor, Wenjian Weng, D.E. Sun. Evaluation of adhesion strength and toughness of fluoridated hydroxyapatite coatings, Thin Solid Films 516 (2008) 5162–5167.

[34] H. Oechsner H, Secondary neutral mass spectrometry (SNMS) and its application to depth profile and interface analysis, In: H. Oechsner H (Ed.), Thin Film and Depth Profile Analysis, Springer-Verlag, Berlin Heidelberg, 1984, pp. 63–85.

[35] L. Péter, G.L. Katona, Z. Berényi, K. Vad, G.A. Langer, E. Tóth-Kádár, J. Pádár, L. Pogány, I. Bakonyi, Electrodeposition of Ni–Co–Cu/Cu multilayers 2. Calculations of the element distribution and experimental depth profile analysis, Electrochim. Acta 53 (2007) 837–845.

[36] X.Y. Liu, P.K. Chu, C.X. Ding, Surface modification of titanium, titanium alloys, and related materials for biomedical applications, Mater. Sci. Eng. R 47 (2004) 49–121.

[37] D. Velten, V. Biehl, F. Aubertin, B. Valeske, W. Possart, J. Breme, Preparation of TiO_2 layers on cp-Ti and Ti6Al4V by thermal and anodic oxidation and by sol-gel coating techniques and their characterization, J. Biomed. Mater. Res. 59 (2002) 18–28.

[38] J. Dai, J. Zhu, C. Chen, F. Weng, High temperature oxidation behavior and research status of modifications on improving high temperature oxidation resistance of titanium alloys and titanium aluminides: A review, J. Alloys Compd. 685 (2016) 784–798.

[39] H.R. Bakhsheshi-Rad, E. Hamzah, M. Daroonparvar, S. N. Saud, M.R. Abdul-kadir, Bi-layer nano-TiO_2/FHA composite coatings on Mg-Zn-Ce alloy prepared by combined physical vapour deposition and electrochemical deposition methods, Vacuum 110 (2014) 127–135.

[40] A. Quirama, A. M. Echavarría, J.M. Meza, J. Osorio, G. Bejarano, Improvement of the mechanical behavior of the calcium phosphate coatings deposited onto Ti6Al4V alloy using an intermediate TiN/TiO_2 bilayer, Vacuum 146 (2017) 22–30.

[41] ISO 13779-4, Implants for surgery-Hydroxyapatite. Part 4. Determination of coating adhesion strength, 2002.

[42] W.C. Wagner, K. Asgar, W.C. Bigelow, R.A. Flinn, Effect of interfacial variables on metal-porcelain bonding, J. Biomed. Mater. Res. 27 (1993) 531–537.

[43] S. Pourhashem, A. Afsharn, Double layer bioglass-silica coatings on 316L stainless steel by sol–gel method, Ceram. Int. 40 (2014) 993–1000.

[44] X. Nie, A. Leyland, A. Matthews, Deposition of layered bioceramic hydroxyapatite/TiO_2 coatings on titanium alloys using a hybrid technique of micro-arc oxidation and electrophoresis, Surf. Coat. Technol. 125 (2000) 407–414.

Figure legends

Fig. 1. Experimental setup of the electrostatic spray deposition technique.

Fig. 2. SEM image from the sediment of the suspension prepared for electrospray deposition. The inert was a higher magnification.

Fig. 3. SEM image (a) and EDX analysis (b) of the as-prepared CaSi coating. Insert shows the surface from 60° tilt angle.

Fig. 4. XRD pattern (a) and Raman spectrum (b) of the as-prepared CaSi coating.

Fig. 5. XRD patterns of all annealed CaSi coatings at different temperatures (1: β-$Ca_2(SiO_4)$; 2: $CaSiO_3$; 3: Ca_3SiO_4; R: rutile).

Fig. 6. SEM images of the CaSi coatings before and after annealing at different temperatures.

Fig. 7. Cross-sectional SEM view (a) and SNMS depth profile (b) of the CaSi coating annealed at 800 °C. The thickness of the layers (d_{Ca} and d_{TiO}) determined by the position of the half interface width (Δx^{Ca} and Δx^{TiO}), which was obtained from the position of the distances between the 90 to 10% decay of measured intensity.

Fig. 8. Open circuit potential against time curves of the as-prepared and annealed CaSi coatings in SBF.

Fig. 9. Typical potentiodynamic polarization curves of the as-prepared and annealed CaSi coatings in SBF.

Table 1

Thickness of the CaSi coating, thickness of oxidation layer, bond strength, and corrosion parameters of the coatings before and after annealing.

Sample	Thickness of CaSi coating (nm)	Thickness of oxidation layer (nm)	Bond strength (MPa)	Corrosion parameter	
				Ecorr (mV)	Icorr (nA/cm^2)
As-prepared	978±61^{a}	10±1^{a}	2.6±0.6^{a}	−595±83^{a}	−67±18^{a}
500 °C	974±72^{a}	57±4^{a,b}	-	-	-
600 °C	1027±73^{a}	185±13^{a,b}	-	-	-
700 °C	1079±77^{a}	377±26^{b}	7.0±3.1^{b}	−431±59^{b}	−22±7^{a}
800 °C	981±76^{a}	1816±134^{c}	9.5±2.9^{b}	−352±58^{b}	−40±14^{a}
900 °C	998±74^{a}	4742±238^{d}	2.5±0.3^{a}	−345±72^{b}	−48±17^{a}
Ti substrate	-	10±1^{a}	-	−567±39^{a}	−186±78^{b}

Mean values followed by the same superscript letter in the same column are not significantly different ($p > 0.05$) according to Scheffe's multiple comparisons.

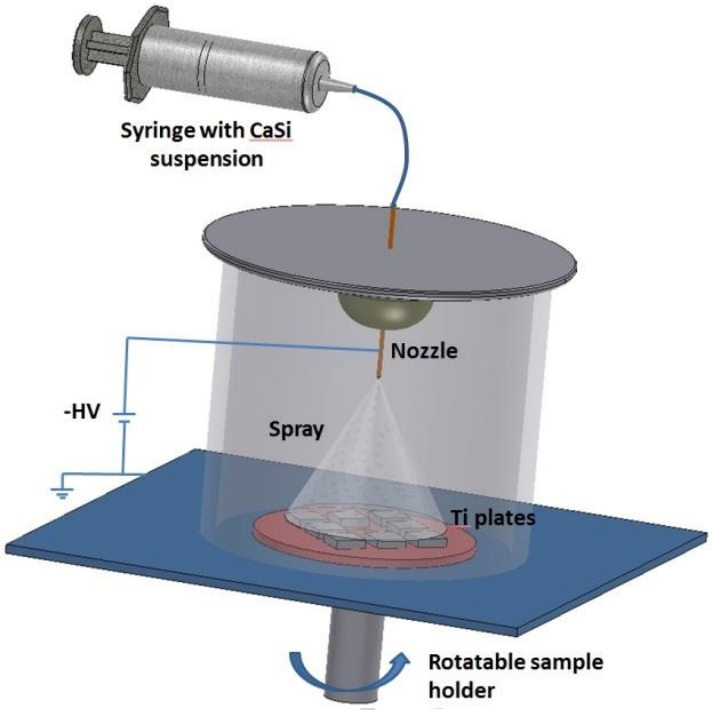

Fig. 1.

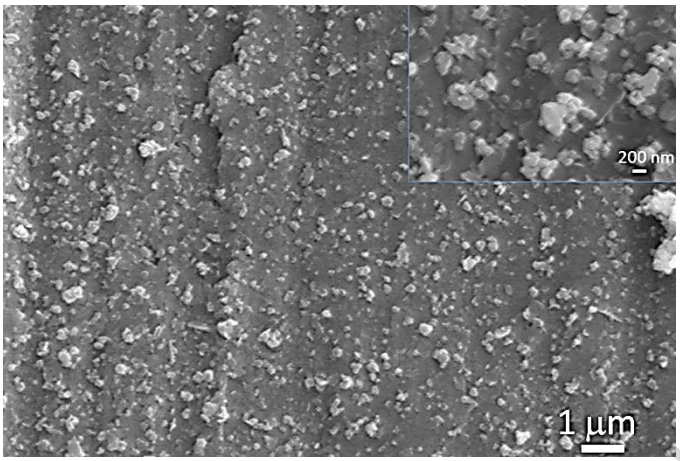

Fig. 2.

a

b

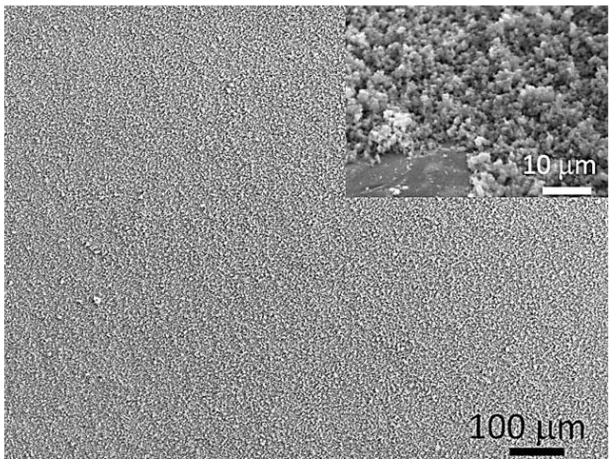

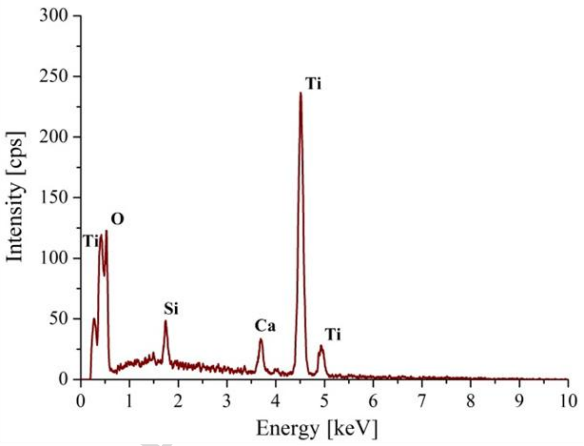

Fig. 3.

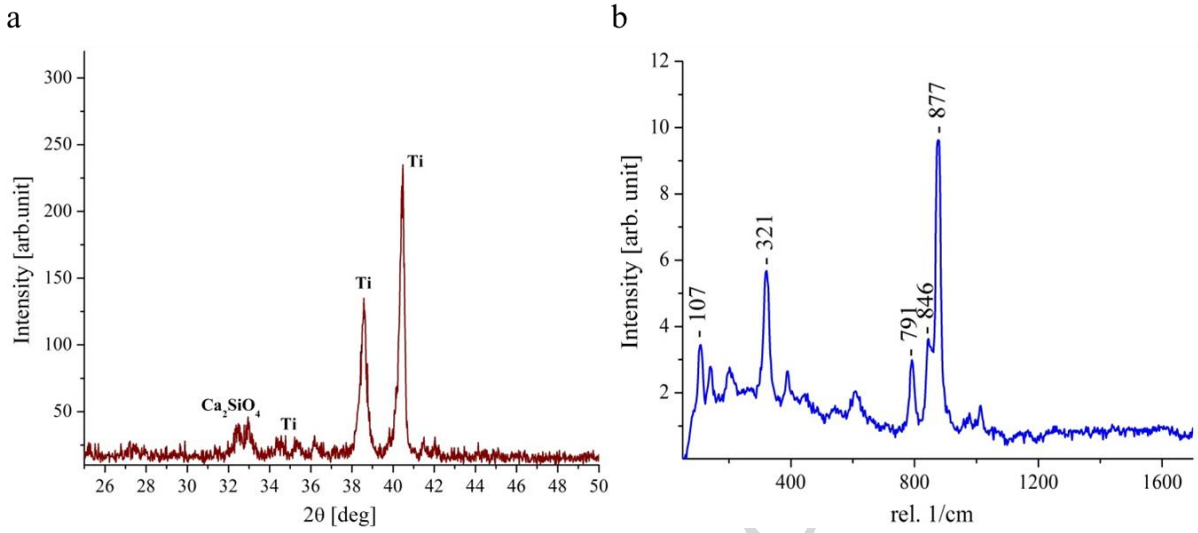

Fig. 4.

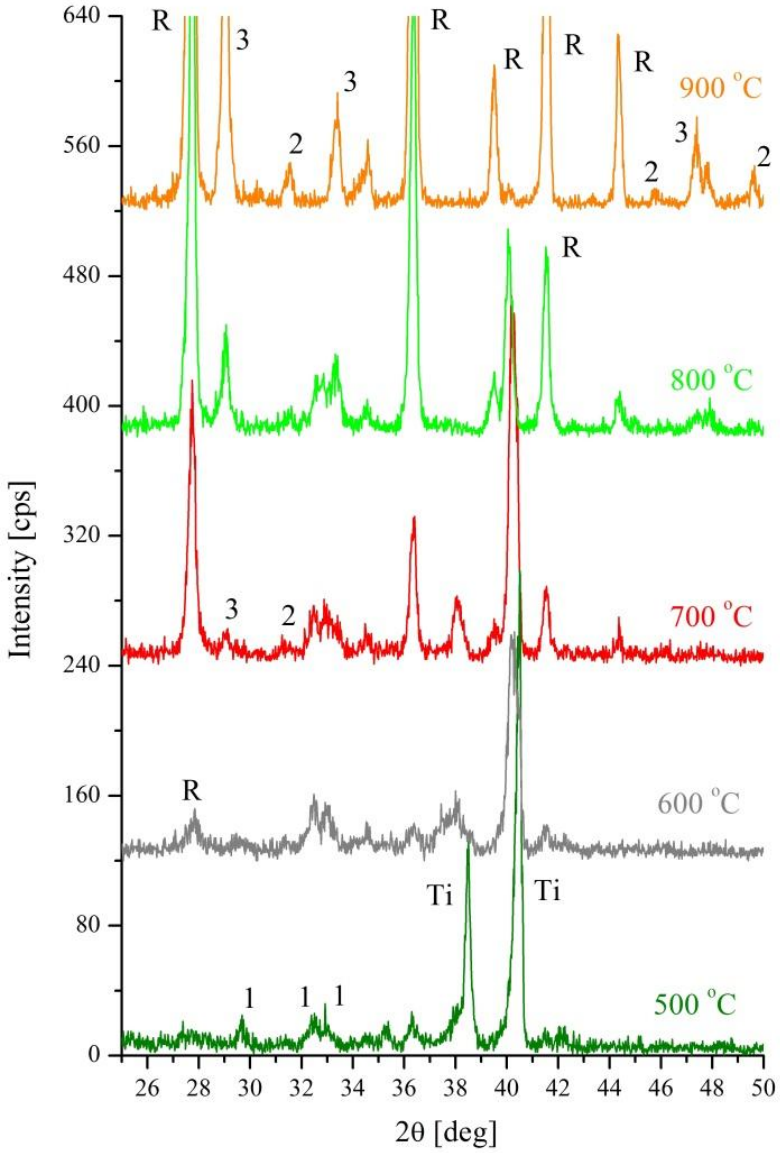

Fig. 5.

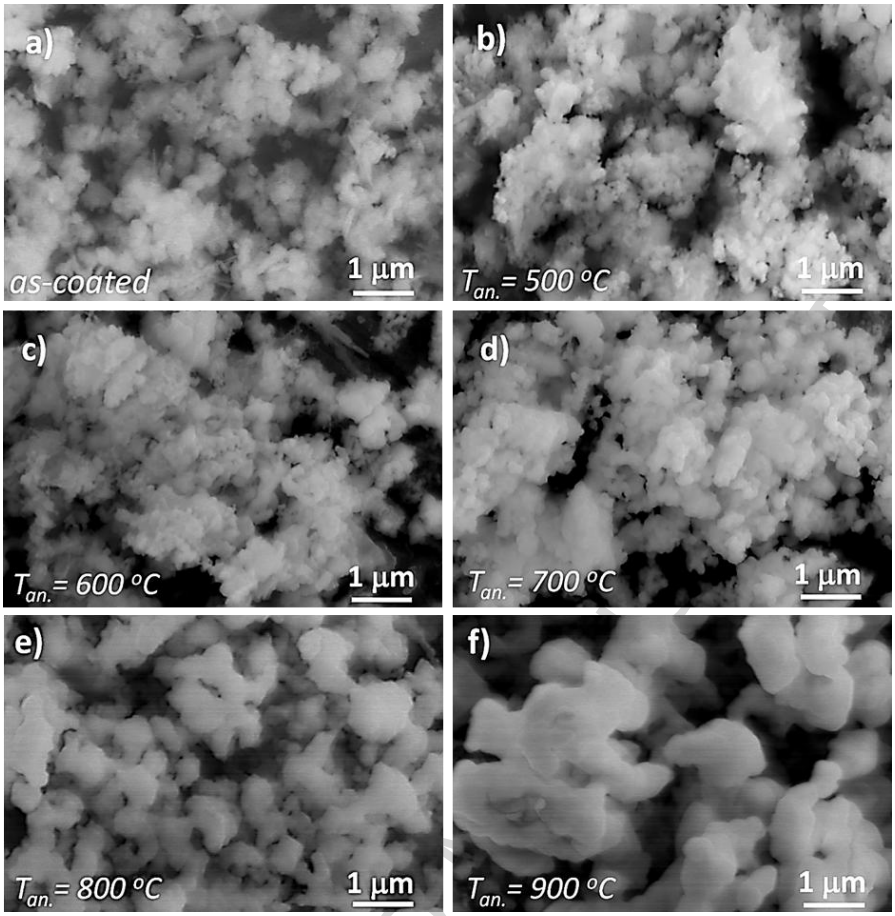

Fig. 6.

a

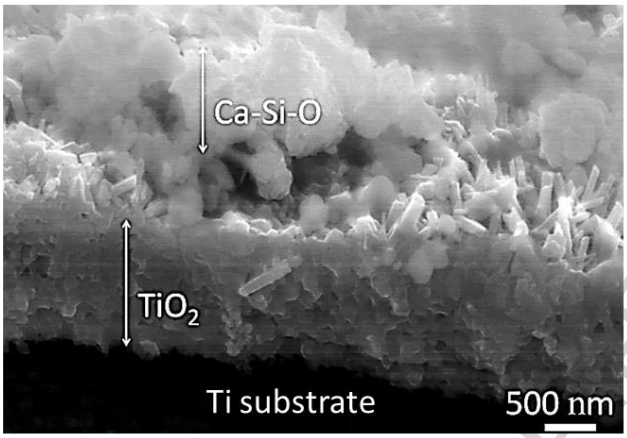

b

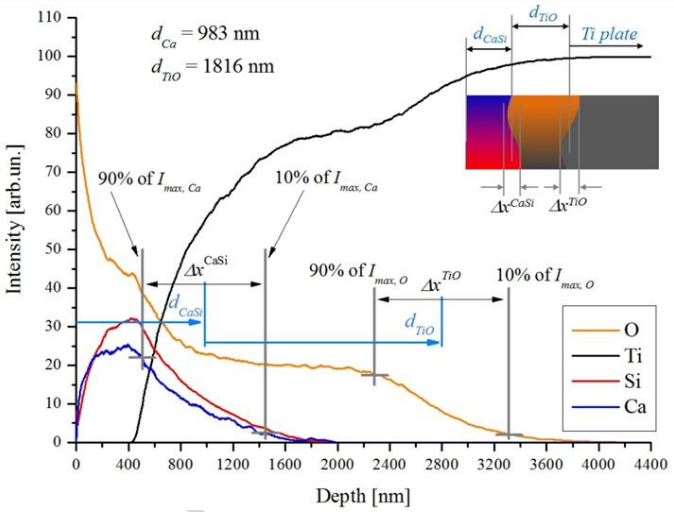

Fig. 7.

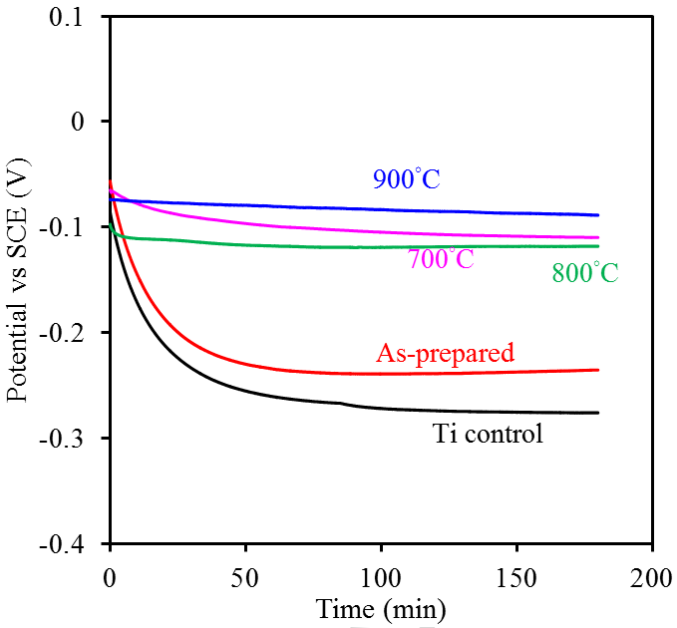

Fig. 8.

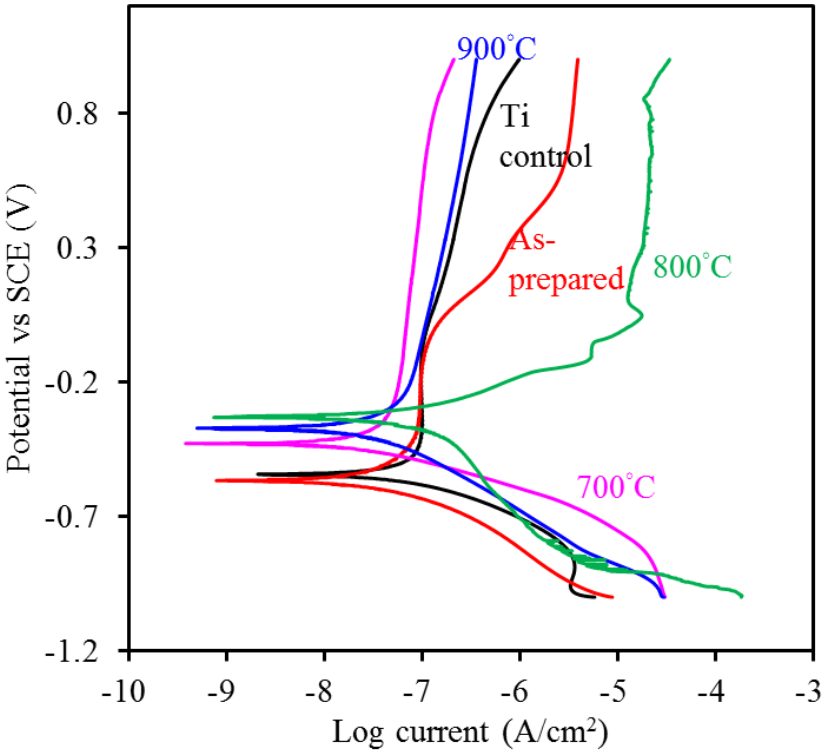

Fig. 9.

Highlights

- It is the first time to coat a homogeneous calcium silicate layer on the Ti substrate by a facile electrospray deposition.
- Annealing of deposited samples in the range of 700−800 °C was effective for the formation of a rutile phase, while maintained the composition of the CaSi material.
- The annealing at temperature of 800 °C achieved the significantly higher bond strength compared to the as-prepared coating.
- The 800 °C-annealed coating had the enhanced corrosion-resistant ability.